

Zhen Wang; Wei Sun; Zhouchao Wei; Shanwen Zhang

Periodic parametric perturbation control for a 3D autonomous chaotic system and its dynamics at infinity

Kybernetika, Vol. 53 (2017), No. 2, 354–369

Persistent URL: <http://dml.cz/dmlcz/146809>

Terms of use:

© Institute of Information Theory and Automation AS CR, 2017

Institute of Mathematics of the Czech Academy of Sciences provides access to digitized documents strictly for personal use. Each copy of any part of this document must contain these *Terms of use*.



This document has been digitized, optimized for electronic delivery and stamped with digital signature within the project *DML-CZ: The Czech Digital Mathematics Library* <http://dml.cz>

PERIODIC PARAMETRIC PERTURBATION CONTROL FOR A 3D AUTONOMOUS CHAOTIC SYSTEM AND ITS DYNAMICS AT INFINITY

ZHEN WANG, WEI SUN, ZHOUCHAO WEI AND SHANWEN ZHANG

Periodic parametric perturbation control and dynamics at infinity for a 3D autonomous quadratic chaotic system are studied in this paper. Using the Melnikov's method, the existence of homoclinic orbits, oscillating periodic orbits and rotating periodic orbits are discussed after transferring the 3D autonomous chaotic system to a slowly varying oscillator. Moreover, the parameter bifurcation conditions of these orbits are obtained. In order to study the global structure, the dynamics at infinity of this system are analyzed through Poincaré compactification. The simulation results demonstrate feasibility of periodic parametric perturbation control technology and correctness of the theoretical results.

Keywords: Hamiltonian system, Melnikov's methods, homoclinic orbits, periodic orbits, periodic parametric perturbation, dynamics at infinity

Classification: 34H10, 34D20, 34H20

1. INTRODUCTION

Since Lorenz equation was found in 1963 [13], many 3D quadratic chaotic systems have been extensively studied and applied in science, engineering, and mathematical communities. Especially, constructing chaotic systems such as Lorenz-like systems, multi-scroll chaotic systems and chaotic systems with hidden attractors etc, has become a research focus in scientific and engineering fields [17]. Meanwhile, the corresponding designing methods, such as state back control technique, nonautonomous technique, and switching function technique, was presented [21]. Extensive research shows that chaotic systems have either self-excited attractors which have a basin of attraction associated with an unstable equilibrium, or hidden attractors with a basin of attraction that does not intersect with small neighborhoods of any equilibrium points [7].

From the view of classification conditions [2], Lorenz system satisfies $a_{12}a_{21} > 0$, and Chen system satisfies $a_{12}a_{21} < 0$. In 2002, Lü presented a transition system which satisfies $a_{12}a_{21} = 0$ between the Lorenz system and the Chen system [14]. In 2008, Yang and Chen described another classification condition for chaotic systems, which are classified into the Lorenz system group, the Chen system group and the Yang-Chen system group (transition system) if $a_{11}a_{22} > 0$, $a_{11}a_{22} < 0$ and $a_{11}a_{22} = 0$. In fact, the

transition system (Yang-Chen system group) has been discussed by Gh. Tigan, Yang and Wang in 2005, 2008, 2010 respectively [20, 23, 25, 33]. Since the transition chaotic system connects the Lorenz attractor and Chen attractor, how to construct a transition system will be an important thing in chaos research. Moreover, The main purpose of studying chaos is to reveal the mechanism of chaos formation, the existence of chaotic attractors, the routes to chaos and the dynamic behaviors of chaos etc. Furthermore, researchers frequently encounter chaos control and chaos synchronization problems in many physical chaotic systems due to the sensitivity of chaos, and they have developed many methods and techniques over the last few decades, such as feedback control, pulse control, adaptive control, passivity control [10, 24, 25, 26] and different kinds of synchronization like complete synchronization (CS, i.e. Identical synchronization (IS)), phase synchronization (PS), lag synchronization (LS), anticipatory synchronization (AS), GS, and multiplexing synchronization (MS) [1, 9]. As we know, the main method used in previous studies is numerical computation, and the qualitative analysis of orbit structure and periodic orbits have not been well studied [6, 18, 22, 29].

To study the periodic solutions of dynamic systems, a new control method based on perturbation theories has been presented in Ref. [15, 16]. In Ref. [4], Melnikov's perturbation was used to explain the control mechanism for Duffing oscillators, Ueda oscillators, and Brusselator oscillators. In Ref. [28, 30], periodic parametric perturbation control method was presented in Lorenz equations and diffusionless Lorenz equations. From the above point of view, we can see that the study of constructing simple chaotic systems and analysis of periodic orbits construct for the systems are of highly practical importance. Following this idea, and from the view of evolutionary dynamics [19], most constructed chaotic systems belong to Lorenz-like systems in accordance with classification conditions. However, transition systems which connect the Lorenz attractors and Chen attractors are rarely mentioned. In 2014, we have proposed one of the transition systems

$$\frac{dx}{dt} = a(y - x), \quad \frac{dy}{dt} = cx - axz, \quad \frac{dz}{dt} = -bz + xy \quad (1)$$

where a, b, c are real parameters in Ref. [27]. Moreover, we studied its invariant algebraic surface and dynamics near finite singularities on the surface in Ref. [27]. In spite of this, more complex dynamics of the transition system (1) need to be investigated, such as the dynamics at infinity and generation mechanism of chaos. Therefore, through the use of the Poincaré compactification of polynomial vector field and Melnikov's method, this paper analyzes dynamics at infinity in the transition system (1), and periodic orbits in the transition system (1) with periodic parametric perturbation.

The paper is organized as follows: In Section 2, the technique of Poincaré compactification is used to investigate the dynamics at infinity of the system (1). In section 3, we reduce the system (1) into a generalized Hamiltonian system with periodic parametric perturbation to get the approximate expressions of homoclinic orbits and periodic orbits. Moreover, the parameter bifurcation conditions of homoclinic orbits and periodic orbits are analyzed and calculated using Melnikov's method in this section. In section 4, numerical simulations are provided to illustrate the performance of the proposed analysis, together with the parameter values chosen for simulations in this section. Finally concluding remarks are given in section 5.

2. DYNAMICS ANALYSIS AT INFINITY

The following lemma shows existence and local stability of fixed points of Eq. (1)

- Lemma 2.1.** 1) The system (1) has only one equilibrium point $O(0, 0, 0)$ if $ab \neq 0$, $c = 0$ or $abc < 0$, and it has three equilibrium points $O(0, 0, 0)$, $E_+(\sqrt{\frac{bc}{a}}, \sqrt{\frac{bc}{a}}, \frac{c}{a})$, $E_-(-\sqrt{\frac{bc}{a}}, -\sqrt{\frac{bc}{a}}, \frac{c}{a})$ if $abc > 0$.
- 2) $O(0, 0, 0)$ is asymptotically stable if $b > 0$, $a > 0$, $c < 0$, $a + 4c \geq 0$.
- 3) If $b < 0$ or $a > 0$, $c > 0$ or $a < 0$, $a + 4c \leq 0$, then $O(0, 0, 0)$ is unstable.
- 4) The equilibrium points E_+ , E_- are asymptotically stable if and only if $a + b > 0$, $abc > 0$ and $a^2b + ab^2 + b^2c - abc > 0$.

In order to make an analysis of the flow of the system (1) at infinity, we use the Poincaré compactification method [3, 11] in this section. Let $S^3 = \{r = (r_1, r_2, r_3, r_4) \in R^4 \mid \|r\| = 1\}$ be a Poincaré unit sphere. We divide this sphere into $S_+ = \{r \in S^3, r_4 > 0\}$ (the northern hemisphere), $S_- = \{r \in S^3, r_4 < 0\}$ (the southern hemisphere) and $S^1 = \{r \in S^3, r_4 = 0\}$ (the equator). Denote the tangent hyperplanes at the point $(\pm 1, 0, 0, 0)$, $(0, \pm 1, 0, 0)$, $(0, 0, \pm 1, 0)$, $(0, 0, 0, \pm 1)$ by the local chart U_i, V_i for $i = 1, 2, 3, 4$, where $U_i = \{r \in S^3, r_i > 0\}$, $V_i = \{r \in S^3, r_i < 0\}$. Define the central projections $f^+ : R^3 \rightarrow S^3$ and $f^- : R^3 \rightarrow S^3$ by

$$f^\pm(x, y, z) = \pm(\frac{x}{\Delta}, \frac{y}{\Delta}, \frac{z}{\Delta}, \frac{1}{\Delta}), \text{ where } \Delta = \sqrt{1 + x^2 + y^2 + z^2},$$

also define $\varphi_k : U_k \rightarrow R^3$, $\phi_k : V_k \rightarrow R^3$ by $\varphi_k = -\phi_k = (\frac{r_l}{r_k}, \frac{r_m}{r_k}, \frac{r_n}{r_k})$ for $k = 1, 2, 3, 4$ with $1 \leq l, m, n \leq 4$ and $l, m, n \neq k$. We only consider the local charts U_i, V_i for $i = 1, 2, 3$ to get the dynamics at x, y, z infinity (shown in Figure 1).

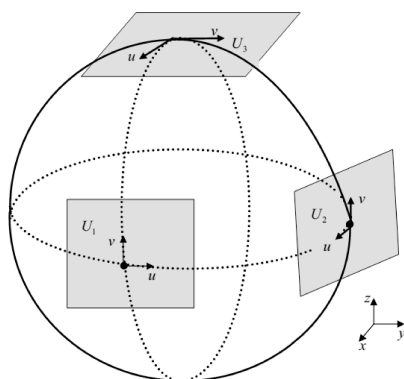


Fig. 1. Orientation of the local charts U_i, V_i for $i = 1, 2, 3$ in the positive endpoints of the x, y, z axis.

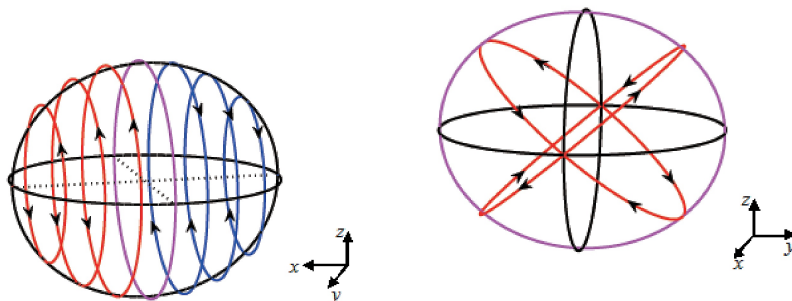


Fig. 2. Phase portrait of the system (1) on the Poincaré sphere at infinity: $a > 0$ (left) and $a < 0$ (right).

Theorem 2.2. For all values of the parameters a , b and c , the phase portrait of the system (1) on the Poincaré sphere at infinity are shown in Figure 2. There exist two centers at the positive and negative of the x axis and a circle of equilibria containing the endpoints of the y axis and the z axis for $a > 0$. But for $a < 0$, there exist two saddles at the positive and negative of the x axis and a circle of equilibria containing the endpoints of the y axis and the z axis. Especially, in the circle of equilibria, there are four linearly zero points, and the stable or unstable manifolds of the saddles at the x axis connecting these linearly zero points.

In the local charts U_1 and V_1 . Take the change of variables $(x, y, z) = (w^{-1}, uw^{-1}, vw^{-1})$ and $t = w\tau$, the system (1) becomes

$$\frac{du}{d\tau} = cw - av + au(w - wu), \quad \frac{dv}{d\tau} = -bvw + u + av(w - wu), \quad \frac{dw}{d\tau} = aw(w - wu). \quad (2)$$

If $w = 0$, the system (2) reduces to

$$\frac{du}{d\tau} = -av, \quad \frac{dv}{d\tau} = u. \quad (3)$$

The system (3) has a unique singularity $(0, 0)$, which is a center for $a > 0$ and a saddle for $a < 0$. The phase portraits are shown in Figure 3.

The flow in the local chart V_1 is the same as the flow in the local chart U_1 reversing the time, hence, the system (1) has a center for $a > 0$ or a saddle for $a < 0$ on the infinite sphere at the negative endpoint of the x axis.

In the local charts U_2 and V_2 . Next, we study the dynamics of the system (1) at infinity of the y axis. Take the transformation $(x, y, z) = (uw^{-1}, w^{-1}, vw^{-1})$ and $t = w\tau$, the system (1) becomes

$$\frac{du}{d\tau} = aw(1-u) + u(auv - cwu), \quad \frac{dv}{d\tau} = u - bvw + v(auv - cwu), \quad \frac{dw}{d\tau} = w(auv - cwu). \quad (4)$$

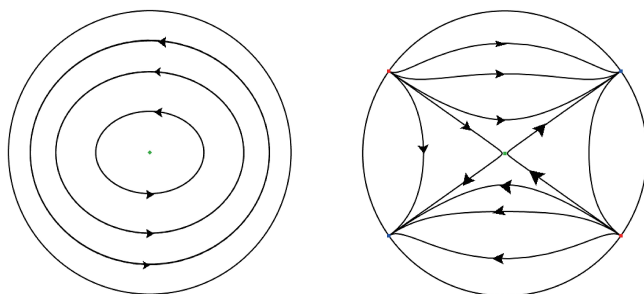


Fig. 3. Phase portraits of the system (1) on the Poincaré sphere at infinity in the local chart U_1 .

If $w = 0$, the system (4) reduces to

$$\frac{du}{d\tau} = au^2v, \quad \frac{dv}{d\tau} = u + auv^2. \tag{5}$$

The system (5) has a line equilibria given by $u = 0$. The singularity $(0, v)$ is a nilpotent singular point as shown in Figure 4 (left) for $a > 0$. If $a < 0$, and $1 + av^2 \neq 0$, $(0, v)$ is a nilpotent singular point, but if $a < 0$ and $1 + av^2 = 0$, $(0, v)$ is a linearly zero. The local phase portrait is shown in Figure 4 (right).

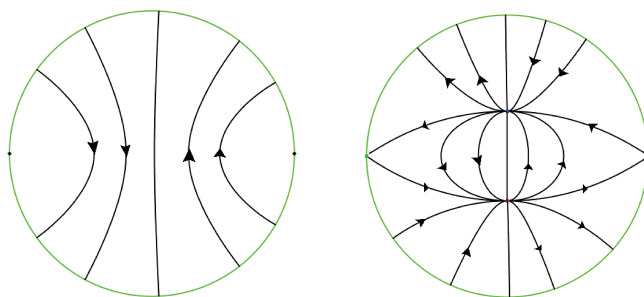


Fig. 4. Phase portraits of the system (1) on the Poincaré sphere at infinity in the local chart U_2 .

The flow in the local chart V_2 is the same as the flow in the local chart U_2 , hence, the phase portrait of the system (1) on the infinite sphere at the negative endpoint of the y axis is shown in Figure 4, reversing the time direction.

In the local charts U_3 and V_3 . Finally, we consider infinity at the z axis. Let $(x, y, z) = (uw^{-1}, vw^{-1}, w^{-1})$ and $t = w\tau$, the system (1) becomes

$$\frac{du}{d\tau} = aw(v - u) + u(bw - uv), \quad \frac{dv}{d\tau} = cvw - au + v(bw - uv), \quad \frac{dw}{d\tau} = w(bw - uv). \tag{6}$$

If $w = 0$, the system (6) reduces to

$$\frac{du}{d\tau} = -u^2v, \frac{dv}{d\tau} = -au - uv^2. \tag{7}$$

The system (7) has a line equilibria given by $u = 0$. The phase portrait of the system (1) at infinity on the local chart U_3 is the same as that in the local chart V_2 for $a > 0$, and is the same as that in the local chart U_2 for $a < 0$. Again the flow in the local chart V_3 is the same as the flow in the local chart U_3 when reversing the time.

From the above analysis, and taking its orientation as shown in Figure 1 into account, we can get the structure of the system (1) on the sphere at infinity shown in Figure 2. We must note that the linearly zero point $(0, \pm\sqrt{\frac{1}{-a}})$ of the system (5) and the linearly zero point $(0, \pm\sqrt{-a})$ of the system (7) are the same points in the space of xyz . From Figure 1, we can see that in the local chart U_2 , the infinity of the v axis is the origin of the v axis in the local chart U_3 , so there exists a reciprocal relation from U_2 to U_3 .

3. PERIODIC PARAMETRIC PERTURBATION CONTROL

For the system (1), let $a = 0.2$, $b = 1$ and $c = 9$, we can find that chaos exists in the system (1) as shown in Figure 5.

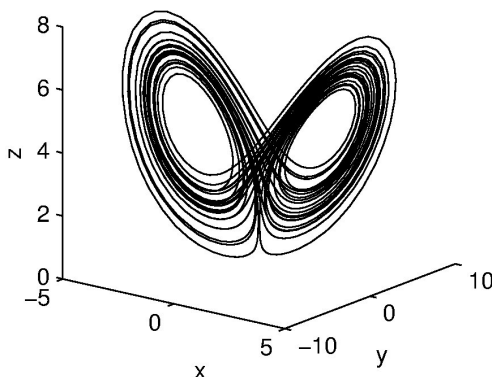


Fig. 5. Chaotic attractor of the system (1).

In order to control chaos of the system (1), let $x = \tilde{x}$, $y = \frac{1}{\sqrt{a}}\tilde{y}$, and $z = \frac{1}{a}(c - \tilde{z})$, then the system can be written as

$$\frac{d\tilde{x}}{dt} = -a\tilde{x} + \sqrt{a}\tilde{y}, \frac{d\tilde{y}}{dt} = \sqrt{a}\tilde{x}\tilde{z}, \frac{d\tilde{z}}{dt} = b(c - \tilde{z}) - \sqrt{a}\tilde{x}\tilde{y}. \tag{8}$$

And using the method of periodic parametric perturbation, we construct a control system

$$\frac{d\tilde{x}}{dt} = -a\tilde{x} + \sqrt{a}\tilde{y}, \frac{d\tilde{y}}{dt} = \sqrt{a}\tilde{x}\tilde{z}, \frac{d\tilde{z}}{dt} = b(c_0 + c_1 \sin \omega t - \tilde{z}) - \sqrt{a}\tilde{x}\tilde{y}. \tag{9}$$

Let $\tilde{x} = \frac{\hat{x}}{\varepsilon}$, $\tilde{y} = \frac{\hat{y}}{\varepsilon^2}$, $\tilde{z} = \frac{\hat{z}}{\varepsilon^2}$, $t = \varepsilon\tau$, $\omega = \frac{\omega_1}{\varepsilon}$, $\varepsilon = \frac{1}{\sqrt{bc_0}}$, then (9) has the form

$$\frac{d\tilde{x}}{d\tau} = \sqrt{a}\tilde{y} - \varepsilon a\tilde{x}, \frac{d\tilde{y}}{d\tau} = \sqrt{a}\tilde{x}\tilde{z}, \frac{d\tilde{z}}{d\tau} = -\sqrt{a}\tilde{x}\tilde{y} + \varepsilon(1 + \frac{c_1}{c_0} \sin \omega_1\tau - b\tilde{z}). \tag{10}$$

Omitting tilde, let $\hat{x} = x$, $\hat{y} = y$, $\hat{z} = z$, $\tau = t$, and using “.” to denote the derivative, the system (10) can be changed into

$$\dot{x} = \sqrt{a}y - \varepsilon ax, \dot{y} = \sqrt{a}xz, \dot{z} = -\sqrt{a}xy + \varepsilon(1 + \frac{c_1}{c_0} \sin \omega_1 t - bz). \tag{11}$$

Obviously, system (11) will become a generalized Hamiltonian system when $\varepsilon = 0$,

$$\begin{pmatrix} \dot{x} \\ \dot{y} \\ \dot{z} \end{pmatrix} = \begin{pmatrix} 0 & -\sqrt{a}z & \sqrt{a}y \\ \sqrt{a}z & 0 & 0 \\ -\sqrt{a}y & 0 & 0 \end{pmatrix} \begin{pmatrix} x \\ y \\ z \end{pmatrix} = J \begin{pmatrix} \frac{\partial H}{\partial x} \\ \frac{\partial H}{\partial y} \\ \frac{\partial H}{\partial z} \end{pmatrix}, \tag{12}$$

where the Hamiltonian function is $H(x, y, z) = \frac{1}{2}x^2 + z = A$, and the Casimir function is $C(x, y, z) = a(y^2 + z^2) = aB^2$. There is a eight-figure homoclinic orbit at the equilibrium point $(0, 0, B)$ on cylindrical surface $y^2 + z^2 = B^2$ in 3D space, also inside and outside this homoclinic orbit are oscillating periodic orbits and rotating periodic orbits in the cylinder $y^2 + z^2 = B^2$ and $\frac{1}{2}x^2 + z = A$ respectively.

To find the bifurcation conditions of homoclinic orbits and periodic orbits of system (11) by the theories of Hamiltonian systems [8] and Melnikov vector function [5, 12], let $x = x, y = -(B + \rho) \sin \theta, z = -(B + \rho) \cos \theta$ and $B > 0, |\frac{\rho}{B}| \ll 1$, then the system (11) will become a special case of slowly varying system [31, 32]

$$\begin{cases} \dot{\theta} = \sqrt{a}x + \varepsilon(\frac{1}{B + \rho}(\sin \theta + \frac{c_1}{c_0} \sin \omega_1 t \sin \theta) + b \cos \theta \sin \theta) \\ \dot{x} = -\sqrt{a}(B + \rho) \sin \theta - \varepsilon ax \\ \dot{\rho} = -\varepsilon(\cos \theta + \frac{c_1}{c_0} \sin \omega_1 t \cos \theta + b(B + \rho)\cos^2 \theta) \end{cases} \tag{13}$$

when $\varepsilon = 0$, system (13) will be a pendulum in plane $\theta - x$, and its Hamiltonian function is $\tilde{H}(\theta, x, \rho) = \sqrt{a}(\frac{1}{2}x^2 - (B + \rho) \cos \theta) = \sqrt{a}A$. Obviously, when $A = (B + \rho)$, there exists a heteroclinic contour in non-perturbation system $(13)_{\varepsilon=0}$, consisting of two heteroclinic orbits connecting $(-\pi, 0)$ and $(\pi, 0)$, and this heteroclinic contour corresponds to the eight-figure homoclinic orbit of the system (11) in the cylinder $y^2 + z^2 = B^2$. Therefore, we can seek the bifurcation conditions of the homoclinic orbit for system (11) by looking for the bifurcation conditions of the heteroclinic contour for system (13). In the cylinder $y^2 + z^2 = B^2$, we can see that two saddle points $(-\pi, 0)$ and $(\pi, 0)$ of the unperturbed system $(13)_{\varepsilon=0}$ correspond to the same point $(0, 0, B)$ of the non-perturbation system $(11)_{\varepsilon=0}$, so we can say that the heteroclinic loop of the unperturbed system $(13)_{\varepsilon=0}$ is a homoclinic orbit $\{\Gamma_{\pm}\}$ connecting the saddle point $(\theta, x, \rho) = (\pi, 0, \rho)$,

$$\begin{cases} \theta_h(t) = \pm 2 \arctan \left(\sinh \left(\sqrt{a(B + \rho)} t \right) \right) \\ x_h(t) = \pm 2 \sqrt{(B + \rho)} \operatorname{sech} \left(\sqrt{a(B + \rho)} t \right). \end{cases} \tag{14}$$

When $-(B + \rho) < A < (B + \rho)$, there exists oscillation periodic orbit $\{\Gamma_o^\kappa\}$

$$\begin{cases} \theta_o(t, \kappa) = 2 \arcsin \left(\kappa \operatorname{sn} \left(\sqrt{a(B + \rho)} t, \kappa \right) \right) \\ x_o(t, \kappa) = 2\kappa\sqrt{B + \rho} \operatorname{cn} \left(\sqrt{a(B + \rho)} t, \kappa \right) \end{cases} \tag{15}$$

where $\kappa^2 = \frac{A+(B+\rho)}{2(B+\rho)}$, period $T_o(\kappa) = \frac{4K(\kappa)}{\sqrt{a(B+\rho)}}$, $\operatorname{sn}(u, \kappa)$ and $\operatorname{cn}(u, \kappa)$ are the Jacobian elliptic functions with the elliptic modulus κ , $K(\kappa)$ denoting the complete elliptic integral of the first kind.

When $A > (B + \rho)$, there exists rotating periodic orbits $\{\Gamma_\pm\}$

$$\begin{cases} \theta_{r\pm}(t, \kappa_1) = \pm 2 \arcsin \left(\operatorname{sn} \left(\frac{\sqrt{a(B + \rho)}}{\kappa_1} t, \kappa_1 \right) \right) \\ x_{r\pm}(t, \kappa_1) = \pm \frac{2\sqrt{(B+\rho)}}{\kappa_1} \operatorname{dn} \left(\frac{\sqrt{a(B+\rho)}}{\kappa_1} t, \kappa_1 \right) \end{cases} \tag{16}$$

where $\kappa_1^2 = (\kappa^2)^{-1} = \frac{2(B+\rho)}{A+(B+\rho)}$, period $T_r(\kappa_1) = \frac{2\kappa_1 K(\kappa_1)}{\sqrt{a(B+\rho)}}$, and $\operatorname{dn}(u, \kappa)$ is the Jacobian elliptic functions with the elliptic modulus κ .

3.1. Homoclinic orbits analysis

Define the Melnikov function[18,19] for the system (13)

$$\begin{aligned} M_0 &= \int_{-\infty}^{+\infty} \left\{ \begin{array}{l} -a\sqrt{a}x_h^2 + \sqrt{a}\sin^2\theta_h + b\sqrt{a}(B + \rho) \cos \theta_h \sin^2\theta_h \\ + \sqrt{a}\frac{c_1}{c_0} \sin \omega_1 t_0 \sin^2\theta_h \cos \omega_1 t \end{array} \right\} dt \\ &= -a\sqrt{a}N_1 + \sqrt{a}N_2 + b\sqrt{a}(B + \rho)N_3 + \sqrt{a}\frac{c_1}{c_0} \sin \omega_1 t_0 N_4 \end{aligned} \tag{17}$$

where

$$\begin{aligned} N_1 &= \int_{-\infty}^{+\infty} x_h^2 dt = 8\sqrt{\frac{B + \rho}{a}}, \quad N_2 = \int_{-\infty}^{+\infty} \sin^2\theta_h dt = \frac{8}{3\sqrt{a(B + \rho)}}, \\ N_3 &= \int_{-\infty}^{+\infty} \sin^2\theta_h \cos \theta_h dt = \frac{-8}{15\sqrt{a(B + \rho)}}, \\ N_4 &= \int_{-\infty}^{+\infty} \sin^2\theta_h \cos \omega_1 t dt = \frac{4\omega_1\pi}{a(B + \rho) \sinh \frac{\omega_1\pi}{2\sqrt{a(B+\rho)}}} \left(\frac{1}{3} - \frac{\omega_1^2}{6a(B + \rho)} \right). \end{aligned}$$

Hence,

$$\begin{aligned} M_0 &= -8a\sqrt{B + \rho} + \frac{8}{3\sqrt{B + \rho}} - \frac{8b\sqrt{B + \rho}}{15} \\ &+ \frac{c_1}{c_0} \sin \omega_1 t_0 \frac{4\omega_1\pi}{\sqrt{a}(B + \rho) \sinh \frac{\omega_1\pi}{2\sqrt{a(B+\rho)}}} \left(\frac{1}{3} - \frac{\omega_1^2}{6a(B + \rho)} \right). \end{aligned} \tag{18}$$

Theorem 3.1. The system (11) exists two homoclinic orbits in the cylinder $y^2 + z^2 = 1$ nearby the homoclinic orbit $\{\Gamma_{\pm}\}$ of the unperturbed system $(13)_{\varepsilon=0}$ connecting the saddle point $(\theta, x, \rho) = (\pi, 0, \rho)$ when $b = 5 - 15a$.

Proof. When $c_1 = 0$ or $\frac{\omega_1^2}{a(B+\rho)} = 2$, we can see that $M_0 = 0$ from Eq.(18),and has $B + \rho = \frac{5}{15a+b}$. Moreover, if $\rho = 0$, there is $B = \frac{5}{15a+b}$, i.e. $M_0(B) = 0$ but $\frac{\partial M_0}{\partial B} \Big|_{B=\frac{5}{15a+b}} \neq 0$, so there exist two transversal intersection homoclinic orbits. When $c_1 \neq 0$ and $\frac{\omega_1^2}{a(B+\rho)} \neq 2$, the condition of transversal intersection of two homoclinic orbits is

$$\left| \frac{[4 - (12a + \frac{4}{3}b)(B + \rho)]c_0\sqrt{a(B + \rho)} \sinh \frac{\omega_1\pi}{2\sqrt{a(B+\rho)}}}{c_1\omega_1\pi \left(2 - \frac{\omega_1^2}{a(B+\rho)}\right)} \right| < 1.$$

Take $\rho = 0$, $B = 1$, and let $M_0 = 0$, then the parameter bifurcation value of homoclinic orbits is $b = 5 - 15a$. □

3.2. Periodic orbits analysis

In the following, we introduce a subharmonic Melnikov vector function of non-perturbation periodic orbits and the function satisfies $mT = nT_p$ for the analysis of periodic orbits of the system (13)

$$M_1^p = \int_0^{mT} \left\{ \begin{array}{l} -a\sqrt{a}x_p^2 + \sqrt{a}\sin^2\theta_p + b\sqrt{a}(B + \rho) \cos \theta_p \sin^2\theta_p \\ + \sqrt{a}\frac{c_1}{c_0} \sin \omega_1 t_0 \sin^2\theta_p \cos \omega_1 t \end{array} \right\} dt \tag{19}$$

$$M_3^p = \int_0^{mT} [\cos \theta_p + b(B + \rho)\cos^2\theta_p + \frac{c_1}{c_0} \sin \omega_1 t_0 \cos \theta_p \cos \omega_1 t] dt \tag{20}$$

where $p = o$ denoting oscillation periodic orbit, and $p = r$ denoting rotating periodic orbits.

3.2.1. Oscillating periodic orbits analysis

Since the period of oscillating periodic orbits $\{\Gamma_o^\kappa\}$ is $T_o(\kappa) = \frac{4K(\kappa)}{\sqrt{a(B+\rho)}} = \frac{m}{n} \frac{2\pi}{\omega_1} = \frac{m}{n} T$, take $p = o$, and $n = 1$, we have

$$M_1^o = -a\sqrt{a}U_1 + \sqrt{a}U_2 + b\sqrt{a}(B + \rho)U_3 + \sqrt{a}\frac{c_1}{c_0} \sin \omega_1 t_0 U_4 \tag{21}$$

where

$$\begin{aligned}
 U_1 &= \int_0^{mT} x_o^2 dt = 16\sqrt{\frac{B+\rho}{a}} [E(\kappa) - (1-\kappa^2)K(\kappa)] \\
 U_2 &= \int_0^{mT} \sin^2\theta_o dt = \frac{16}{3\sqrt{a(B+\rho)}} [(1-\kappa^2)K(\kappa) - (1-2\kappa^2)E(\kappa)] \\
 U_3 &= \int_0^{mT} \sin^2\theta_o \cos\theta_o dt \\
 &= \frac{16}{15\sqrt{a}(\sqrt{B+\rho})^3} \left[\frac{[5(\kappa^2-1)A - 2(\kappa^4 - 3\kappa^2 + 2)(B+\rho)] K(\kappa)}{+ [5(2\kappa^2-1)A - 4(\kappa^4 - \kappa^2 + 1)(B+\rho)] E(\kappa)} \right] \\
 U_4 &= \int_0^{mT} \sin^2\theta_o \cos\omega_1 t dt \\
 &= \frac{4\kappa^2}{\sqrt{a(B+\rho)}} \int_0^{4mK(\kappa)} \left\{ [\operatorname{sn}^2(u, \kappa) - \kappa^2 \operatorname{sn}^4(u, \kappa)] \cos\left(\frac{m\pi}{2nK(\kappa)}u\right) \right\} du
 \end{aligned}$$

$E(\kappa)$ denotes the complete elliptic integral of the second kind. Hence, when

$$\left| \frac{-aU_1 + U_2 + b(B+\rho)U_3}{\frac{c_1}{c_0}U_4} \right| < 1 \tag{22}$$

then $M_1^o = 0$. We can calculate

$$M_3^o = U_5 + b(B+\rho)U_6 + \frac{c_1}{c_0} \sin\omega_1 t_0 U_7 \tag{23}$$

where

$$\begin{aligned}
 U_5 &= \int_0^{mT} \cos\theta_o dt = \frac{4}{\sqrt{a}(\sqrt{B+\rho})^3} [[2(\kappa^2-1)(B+\rho) - A] K(\kappa) + 2(B+\rho)E(\kappa)] \\
 U_6 &= \int_0^{mT} \cos^2\theta_o dt = \frac{4}{3\sqrt{a}(\sqrt{B+\rho})^5} \left[\begin{aligned} & \left[\begin{aligned} & 4(1-\kappa^2)(2-3\kappa^2)(B+\rho)^2 \\ & + 12A(1-\kappa^2)(B+\rho) + 3A^2 \end{aligned} \right] K(\kappa) \\ & - \left[8(1-2\kappa^2)(B+\rho)^2 + 12A(B+\rho) \right] E(\kappa) \end{aligned} \right] \\
 U_7 &= \int_0^{mT} \cos\theta_o \cos\omega_1 t dt \\
 &= \frac{2\kappa^2}{\sqrt{a(B+\rho)}} \int_0^{4K(\kappa)} \frac{E(\kappa) - \kappa'^2 K(\kappa)}{\kappa^2 K(\kappa)} \cos\left(\frac{m\pi}{2K(\kappa)}u\right) du + \frac{2\kappa^2}{\sqrt{a(B+\rho)}} \\
 & \int_0^{4K(\kappa)} \frac{\pi}{\kappa^2 K^2(\kappa)} \sum_{j=1}^{\infty} \left[j \cdot \operatorname{csch}\left(j \cdot \frac{\pi K'(\kappa)}{K(\kappa)}\right) \cdot \cos\left(j \cdot \frac{\pi}{K(\kappa)}u\right) \right] \cos\left(\frac{m\pi}{2K(\kappa)}u\right) du
 \end{aligned}$$

where $\kappa' = \sqrt{1-\kappa^2}$. So, when

$$\left| \frac{U_5 + b(B+\rho)U_6}{\frac{c_1}{c_0}U_7} \right| < 1 \tag{24}$$

then $M_3^o = 0$. Hence, we can obtain the following theorem.

Theorem 3.2. When the parameters of system (9) satisfy (22) and (24), the corresponding subharmonic Melnikov function is zero, and the period of oscillating periodic orbits is $\frac{2m\pi}{\omega_1}$.

3.2.2. Rotating periodic orbits analysis

Since the period of rotating periodic orbits $\{\Gamma_{\pm}\}$ is $T_r(\kappa_1) = \frac{2\kappa_1 K(\kappa_1)}{\sqrt{a(B+\rho)}} = \frac{m}{n} \frac{2\pi}{\omega_1} = \frac{m}{n} T$, take $p = r, n = 1$ and we have

$$M_1^r = -a\sqrt{a}G_1 + \sqrt{a}G_2 + b\sqrt{a}(B+\rho)G_3 + \sqrt{a}\frac{c_1}{c_0} \sin \omega_1 t_0 G_4 \quad (25)$$

where,

$$\begin{aligned} G_1 &= \int_0^{mT} x_r^2 dt = \frac{8}{\kappa_1} \sqrt{\frac{B+\rho}{a}} E(\kappa_1) \\ G_2 &= \int_0^{mT} \sin^2 \theta_r dt = \frac{16}{3\kappa_1^3 \sqrt{a(B+\rho)}} [2(\kappa_1^2 - 1)K(\kappa_1) - (\kappa_1^2 - 2)E(\kappa_1)] \\ G_3 &= \int_0^{mT} \sin^2 \theta_r \cos \theta_r dt \\ &= \frac{8}{15\kappa_1^5 \sqrt{a}(\sqrt{B+\rho})^3} \left[\begin{aligned} &[10\kappa_1^2(1 - \kappa_1^2)A - 2(\kappa_1^4 - 3\kappa_1^2 + 2)(B + \rho)] K(\kappa_1) \\ &+ [4(\kappa_1^4 - \kappa_1^2 + 1)(B + \rho) - 5\kappa_1^2(2 - \kappa_1^2)A] E(\kappa_1) \end{aligned} \right] \\ G_4 &= \int_0^{mT} \sin^2 \theta_r \cos \omega_1 t dt \\ &= \int_0^{mT} \left\{ 4\text{sn}^2 \left(\frac{\sqrt{a(B+\rho)}}{\kappa_1} t, \kappa_1 \right) \left[1 - \text{sn}^2 \left(\frac{\sqrt{a(B+\rho)}}{\kappa_1} t, \kappa_1 \right) \right] \cos \omega_1 t \right\} dt \end{aligned}$$

Hence, when

$$\left| \frac{-aG_1 + G_2 + b(B+\rho)G_3}{\frac{c_1}{c_0} G_4} \right| < 1 \quad (26)$$

we have $M_1^r = 0$. Also, we can calculate

$$M_3^r = G_5 + b(B+\rho)G_6 + \frac{c_1}{c_0} \sin \omega_1 t_0 G_7 \quad (27)$$

$$\begin{aligned} G_5 &= \int_0^{mT} \cos \theta_r dt = \frac{2}{\kappa_1 \sqrt{a}(\sqrt{B+\rho})^3} [2(B+\rho)E(\kappa_1) - A\kappa_1^2 K(\kappa_1)] \\ G_6 &= \int_0^{mT} \cos^2 \theta_r dt \\ &= \frac{2}{3\kappa_1^3 \sqrt{a}(\sqrt{B+\rho})^5} \left[\begin{aligned} &[4(\kappa_1^2 - 1)(B + \rho)^2 + 3A^2 \kappa_1^4] K(\kappa_1) \\ &+ [8(2 - \kappa_1^2)(B + \rho)^2 + 12\kappa_1^2(B + \rho)] E(\kappa_1) \end{aligned} \right] \end{aligned}$$

$$G_7 = \int_0^{mT} \cos \theta_r \cos \omega_1 t dt = \int_0^{mT} \frac{\frac{2}{\kappa_1^2}(B + \rho) \operatorname{dn}^2 \left(\frac{\sqrt{a(B+\rho)}}{\kappa_1} t, \kappa_1 \right) - A}{B + \rho} \cos \omega_1 t dt$$

Hence, when

$$\left| \frac{G_5 + b(B + \rho)G_6}{\frac{c_1}{c_0}G_7} \right| < 1 \tag{28}$$

then $M_3^T = 0$. Hence, we can obtain the following theorem.

Theorem 3.3. When the parameters of system (9) satisfy (26) and (28), the corresponding subharmonic Melnikov function is zero, and the period of rotating periodic orbits is $\frac{2m\pi}{\omega_1}$.

4. SIMULATION RESULTS

To verify the theoretical derivation and explore the effect of control, numerical simulations for the system (9) are carried out. Take $a = 0.2$, the eight-figure homoclinic orbits, oscillating periodic orbits and rotating periodic orbits of the unperturbed system are shown in Figure 6.

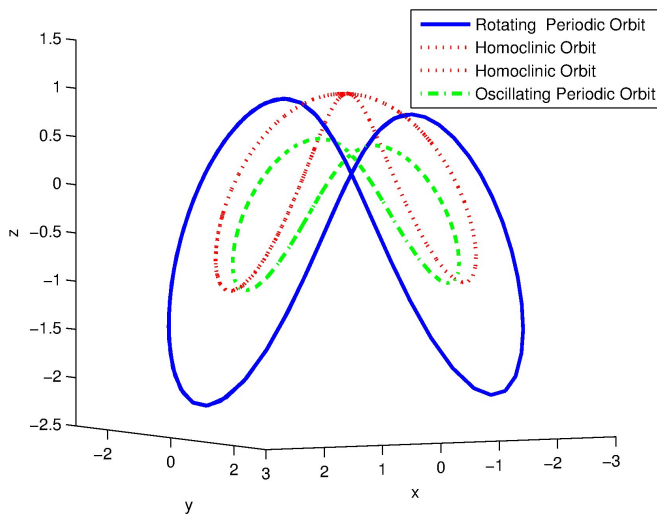


Fig. 6. Homoclinic orbits, oscillating periodic orbits and rotating periodic orbits of unperturbed system $(11)_{\epsilon=0}$ in 3D space (dot line: Homoclinic orbit, dot-dash line: Oscillating periodic orbits and real line: Rotating periodic orbits).

The homoclinic orbit on the space cylinder will become a heteroclinic orbit on the plane $\theta - x$ when the system (11) changes into slowly varying system (13). The heteroclinic orbit of the system (13) and its projection in the 2D plane are shown in Figure 7

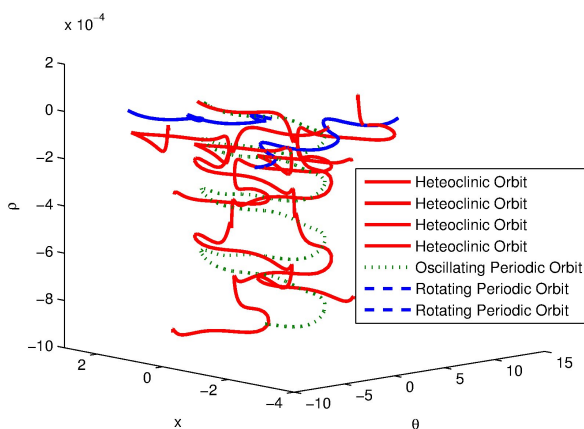


Fig. 7. The heteroclinic orbits, oscillating periodic orbits and rotating periodic orbits of the system (7) in 3D space (dot line: Oscillating periodic orbits, dash line: Rotating periodic orbits and real line: Heteroclinic orbit).

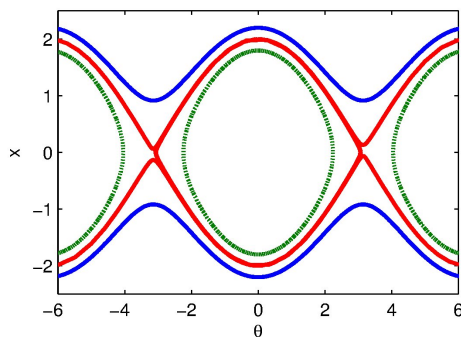


Fig. 8. The projection of the heteroclinic orbits, oscillating periodic orbits and rotating periodic orbits of the system (13) in $\theta - x$ plane.

and Figure 8 respectively. From the Figure 8, we can see that the system (13) exists heteroclinic orbits in 3D space under the condition of parameter bifurcation which were given in theorem 3.1, theorem 3.2, and theorem 3.3 when ε sufficiently close to zero. These heteroclinic orbits correspond to the homoclinic orbits of the system (11). Also under the same conditions, the system will exist oscillating periodic orbits and rotating periodic orbits inside and outside the heteroclinic orbit.

5. CONCLUSION

In this paper, a 3D autonomous chaotic system with periodic parametric perturbation has been reduced to a slowly varying system which is a Hamiltonian perturbed system. The dynamics at infinity of this system has been analyzed by using the Poincaré compactification technique. Moreover, the existence of homoclinic orbit, oscillating periodic orbit and rotating periodic orbit for this perturbed system have been proved by using the generalized Melnikov's method. We have obtained the parameter conditions for these orbits through rigorous symbolic computations. And the homoclinic orbit, the oscillating orbit and the rotating orbit have been displayed by numerical simulation. Future work on the topic should include a theoretical analysis of the dynamics of the perturbed system, in-depth studies of chaos synchronization control and applications in secure communication for this system.

ACKNOWLEDGEMENT

The authors acknowledge the referees and the editor for carefully reading this paper and suggesting many helpful comments. This work was supported by the Natural Science Foundation of China (No.61473237, 11401543), the Natural Science Basic Research Plan in Shaanxi Province of China (No. 2016JM1024), the Scientific Research Program Funded by Shaanxi Provincial Education Department (No.15JK2181), Shaanxi Key Laboratory of Complex System Control and Intelligent Information Processing (No. 2016CP06), Xi'an University of Technology and the Scientific Research Foundation of Xijing University (Grant No.XJ160142), the Open Foundation for Guangxi Colleges and Universities Key Lab of Complex System Optimization and Big Data Processing (No.2016CSOBDP0202), and the Fundamental Research Funds for the Central Universities, China University of Geosciences (Wuhan) (No. CUGL150419).

(Received April 11, 2015)

REFERENCES

- [1] Y. Chen, L. Cao and M. Sun: Robust modified function projective synchronization in network with unknown parameters and mismatch parameters. *Int. J. Nonlinear Sci.* *10* (2010), 17–23.
- [2] S. Čelikovský and A. Vaněček: Bilinear systems and chaos. *Kybernetika* *30* (1994), 403–424.
- [3] F. Dumortier, J. Llibre, and J.C. Artes: *Qualitative Theory of Planar Differential Systems*. Springer, Berlin 2006.
- [4] Y. Y. Fang, Z. Y. Xu and C. H. Cai: Melnikov analysis of feedback control of chaotic dynamics system. *J. Wuxi University of Light Industry* *20* (2001), 624–629.
- [5] J. Guckenheimer and P. Holmes: *Nonlinear Oscillations, Dynamical Systems, and Bifurcations of Vector Fields*. Springer, Berlin 2002. DOI:10.1007/978-1-4612-1140-2
- [6] S. Jafari and J. C. Sprott: Simple chaotic flows with a line equilibrium. *Chaos, Solitons and Fractals* *57* (2013), 79–84. DOI:10.1016/j.chaos.2013.08.018
- [7] A. P. Kuznetsov, S. P. Kuznetsov, and N. V. Stankevich: A simple autonomous quasiperiodic self-oscillator. *Commun. Nonlinear Sci. Numer. Simul.* *15* (2010), 1676–1681. DOI:10.1016/j.cnsns.2009.06.027

- [8] J. B. Li, X. H. Zhao, and Z. R. Liu: Theory of Generalized Hamiltonian System and its Applications. Science Press, Beijing 2007.
- [9] Y. Li, X. Q. Wu, J. A. Lu, and J. H. Lü: Synchronizability of duplex networks. IEEE Trans. Circuits and Systems II *63* (2016), 206–210. DOI:10.1109/tcsii.2015.2468924
- [10] K. X. Liu, L. L. Wu, J. H. Lü and H. H. Zhu: Finite-time adaptive consensus of a class of multi-agent systems. Science China-Technological Sciences *59* (2016), 22–32. DOI:10.1007/s11431-015-5989-7
- [11] Y. J. Liu: Analysis of global dynamics in an unusual 3D chaotic system. Nonlinear Dyn. *70* (2012), 2203–2212. DOI:10.1007/s11071-012-0610-0
- [12] Z. R. Liu: Perturbation Criteria for Chaos. Shanghai Scientific and Technological Education Publishing House, Shanghai 1994.
- [13] E. N. Lorenz: Deterministic non-periodic flow. J. Atmospheric Sci. *20* (1963), 130–141. DOI:10.1175/1520-0469(1963)020<0130:dnfj>2.0.co;2
- [14] J. H. Lü and G. R. Chen: A new chaotic attractor coined. Int. J. Bifurcation and Chaos *12* (2002), 659–661. DOI:10.1142/s0218127402004620
- [15] K. A. Mirus and J. C. Sprott: Controlling chaos in a high dimensional systems with periodic parametric perturbations. Phys. Lett. A *254* (1999), 275–278. DOI:10.1016/s0375-9601(99)00068-7
- [16] K. A. Mirus and J. C. Sprott: Controlling chaos in low- and high-dimensional systems with periodic parametric perturbations. Phys. Rev. E *59* (1999), 5313–5324. DOI:10.1103/physreve.59.5313
- [17] C. W. Shen, S. M. Yu, J. H. Lü, and G. R. Chen: Constructing hyperchaotic systems at will. Int. J. Circuit Theory Appl. *43* (2015), 2039–2056. DOI:10.1002/cta.2062
- [18] J. C. Sprott: Some simple chaotic flows. Phys. Rev. E *50* (1994), 647–650. DOI:10.1103/physreve.50.r647
- [19] S. L. Tan, J. H. Lü, and D. J. Hill: Towards a theoretical framework for analysis and intervention of random drift on general networks. IEEE Trans. Automat. Control *60* (2015), 576–581. DOI:10.1109/tac.2014.2329235
- [20] G. Tigan: Analysis of a dynamical system derived from the Lorenz system. Scientific Bull. Politehnica University of Timisoara *50* (2005), 61–72.
- [21] Q. X. Wang, S. M. Yu, C. Q. Li, J. H. Lü, X. L. Fang, and J. M. Bahi: Theoretical design and FPGA-based implementation of higher-dimensional digital chaotic systems. IEEE Trans. Circuits and Systems I *63* (2016), 401–412. DOI:10.1109/tcsi.2016.2515398
- [22] X. Wang and G. R. Chen: Constructing a chaotic system with any number of equilibria. Nonlinear Dynamics *71* (2013), 429–436. DOI:10.1007/s11071-012-0669-7
- [23] Z. Wang: Existence of attractor and control of a 3D differential system. Nonlinear Dynamics *60* (2010), 369–373. DOI:10.1007/s11071-009-9601-1
- [24] Z. Wang: Passivity control of nonlinear electromechanical transducer chaotic system. Control Theory Appl. *28* (2011), 1036–1040.
- [25] Z. Wang, Y. X. Li, X. J. Xi, and L. Lü: Heteroclinic orbit and backstepping control of a 3D chaotic system. Acta Phys. Sin. *60* (2011), 010513.
- [26] Z. Wang, W. Sun, Z. C. Wei and X. J. Xi: Dynamics analysis and robust modified function projective synchronization of Sprott E system with quadratic perturbation. Kybernetika *50* (2014), 616–631. DOI:10.14736/kyb-2014-4-0616

- [27] Z. Wang, Z. C. Wei, X. J. Xi, and Y. X. Li: Dynamics of a 3D autonomous quadratic system with an invariant algebraic surface. *Nonlinear Dynamics* 77 (2014), 1503–1518. DOI:10.1007/s11071-014-1395-0
- [28] Z. C. Wei and Q. G. Yang: Controlling the diffusionless Lorenz equations with periodic parametric perturbation. *Comput. Math. Appl.* 58 (2009), 1979–1987. DOI:10.1016/j.camwa.2009.07.058
- [29] Z. C. Wei, W. Zhang, Z. Wang, and M. H. Yao: Hidden attractors and dynamical behaviors in an extended Rikitake system. *Int. J. Bifurcation and Chaos* 22 (2015), 1550028. DOI:10.1142/s0218127415500285
- [30] Z. M. Wu, J. Y. Xie, Y. Y. Fang, and Z. Y. Xu: Controlling chaos with periodic parametric perturbations in Lorenz system. *Chaos Solitons and Fractals* 32 (2007), 104–112. DOI:10.1016/j.chaos.2005.10.060
- [31] S. Wiggins and P. Holmes: Homiclinic orbits in slowly varying oscillators. *SIAM J. Math. Anal.* 18 (1987), 612–629. DOI:10.1137/0518047
- [32] S. Wiggins and P. Holmes: Periodic orbits in slowly varying oscillators. *SIAM J. Math. Anal.* 18 (1987), 592–611. DOI:10.1137/0518046
- [33] Q. G. Yang and G. R. Chen: A chaotic system with one saddle and two stable node-foci. *Int. J. Bifur. Chaos* 18 (2008), 1393–1414. DOI:10.1142/s0218127408021063

Zhen Wang, *Department of Applied Science, Xijing University, Xi'an 710123 and Shaanxi Key Laboratory of Complex System Control and Intelligent Information Processing, Xi'an University of Technology, Xi'an 710048. P. R. China.*
e-mail: williamchristian@163.com

Wei Sun, *Department of Applied Science, Xijing University, Xi'an 710123. P. R. China.*
e-mail: sunwei@xijing.edu.cn

Zhouchao Wei, *Corresponding author. School of Mathematics and Physics, China University of Geosciences, Wuhan 430074 and Guangxi Colleges and Universities Key Laboratory of Complex System Optimization and Big Data Processing, Yulin Normal University, Yulin, 537000. P. R. China.*
e-mail: weizhouchao@163.com

Shanwen Zhang, *Department of Applied Science, Xijing University, Xi'an 710123. P. R. China.*
e-mail: zhangshanwen@xijing.edu.cn